Improving Biohydrogen Production Using *Clostridium beijerinckii* Immobilized with Magnetite Nanoparticles

Trevor Seelert[1†], Dipankar Ghosh[2†], and Vivian Yargeau[1*]

[1] Department of Chemical Engineering, McGill University, 3610 University St., Montréal, Québec, H3A 2B2, Canada

[2] Département de Microbiologie et Immunologie, Université de Montréal, C.P. 6128, Succ. Centre-ville, Montréal, Québec, H3C 3J7, Canada

* *Corresponding author: viviane.yargeau@mcgill.ca*

† *Both authors equally contributed to this work*

Abstract

In order to supplement the need for alternative energy resources within the near future, enhancing the production of biohydrogen with immobilized *Clostridium beijerinckii* NCIMB8052 was investigated. Magnetite nanoparticles were functionalized with chitosan and alginic acid polyelectrolytes by a layer-by-layer method to promote bacterial attachment. Cultivating *C. beijerinckii* with these nanoparticles resulted in a shorter lag growth phase and increased total biohydrogen production within 100 ml, 250 ml and 3.6 L reactors compared with freely suspended organisms. The greatest hydrogen yield was obtained in the 250 ml reactor of 2.1 (± 0.7) mol H_2/ mol glucose with substrate conversion and energy conversion efficiencies of 52 (±18) % and 10 (±3) % respectively. The hydrogen yields produced are comparable to those

presented in literature, however process improvements are required to increase these substrate and energy conversion efficiencies.

Keywords: Biohydrogen, *Clostridium beijerinckii*, Magnetite, Chitosan, Alginic acid, Immobilization

Introduction

The global population's energy and carbon usage has increased significantly in recent years (Pielke et al. 2008), while current projections indicate energy consumption will increase another 35% by 2035 compared to 2008. Of this future energy demand, countries outside the Organization for Economic Cooperation and Development (OECD) are expected to contribute an 85% increase in their energy usage. The majority of this energy is derived from oil and coal resources (Conti and Holtberg 2011) and thus their use increases the atmospheric CO_2 concentrations, contributing to global climate change (Kothari et al. 2010). As a result, alternative energy resources with minimal atmospheric carbon contributions should be investigated to help offset future global energy needs. Finding such alternative resources would accomplish two significant objectives. First, atmospheric carbon emissions would be reduced, decreasing the overall impact on global climate change. Secondly, an alternative energy resource for non-OECD countries would help lower the environmental footprint between nations. These factors would thus be creating a more sustainable global energy market (Cranston and Hammond 2010). Renewable energy resources typically produce fewer carbon emissions and thus have a smaller environmental impact (Conti and Holtberg 2011; Cullen and Allwood 2010). Utilizing such resources as Nuclear, hydroelectric, wind, geothermal and hydrogen production are some of the potential renewable energy sources in the global market. However, most of these technologies cannot currently produce energy at an economically competitive rate compared with typical carbon intensive processes (Conti and Holtberg 2011). Nuclear and wind energy in particular have received increased focus in recent years. However, both technologies also have significant industrial scale drawbacks. Many countries are experiencing increased concerns regarding nuclear safety and radioactive waste disposal following the accident at the Fukushima

Daiichi plant in March 2011 (Conti and Holtberg 2011; Hayashi and Hughes 2013). Subsequently, wind is considered an intermittent source, hindering the technology's economical value as power may not be available when it is required most (Conti and Holtberg 2011). Hydrogen is thus considered a strong alternative fuel source. It has the largest energy density per unit mass of all known fuels (142 kJ/g) (Ghosh and Hallenbeck 2014) and is considered a "clean fuel" as water is its primary byproduct (Brentner et al. 2010). At present, 95% of hydrogen is produced through fossil fuel dependent processes, primarily steam methane reforming of natural gas (Brentner et al. 2010). Other such processes include thermal cracking of natural gas, partial oxidation of hydrocarbons and coal gasification (Hallenbeck and Ghosh 2009). Most other hydrogen is produced as a by-product of chemical processes with water electrolysis contributing a small amount (Brentner et al. 2010). However, not only do the majority of the above processes rely on non-renewable fossil fuel resources, but they also occur at high temperatures or pressures and are thus energy intensive (Hallenbeck and Ghosh 2009). Hydrogen production through biological processes (biohydrogen) is an alternative production scheme based solely on various renewable resources. Biohydrogen production does not rely on fossil fuels, is typically performed at moderate temperatures and is considered carbon neutral; therefore it has a no net increase in carbon emissions. As a result, if biohydrogen can be produced in an economically feasible manner, it can be an important alternative to current fuel sources.

Biohydrogen is typically produced through one of four processes, biophotolysis of water, indirect biophotolysis, photofermentation and dark fermentation. There are pros and cons to each method, however biophotolysis and indirect biophotolysis have low photochemical efficiencies (Brentner et al. 2010; Hallenbeck and Ghosh 2009), while photofermentation systems do not currently produce hydrogen at a competitive rate (Brentner et al. 2010). Dark fermentation is

performed by anaerobic organisms (strict and facultative) such as *Clostridium beijerinckii*. This process is often accompanied by low substrate conversion efficiency due to competing metabolic pathways as outlined in **Error! Reference source not found.**. However, dark fermentation also produces the highest volumetric amount of hydrogen between each process. As there are also numerous areas for improvement including immobilizing microorganisms, optimizing process conditions and genetically modifying organisms, dark fermentation processes also have the potential for significant improvement.

Immobilizing microorganisms on solid substrates retains biomass within reactors which has been shown to increase volumetric hydrogen production (Bartacek et al. 2007). Therefore, a novel immobilization technique has been investigated, utilizing super paramagnetic nanoparticles (NPs) as the solid substrate for attachment. Using a substrate of this nature would allow organisms to be retained from batch to batch by applying a magnetic field. This magnetic field separates biomass from the liquid media, allowing fresh liquid to be added to begin a new growth and production phase. *Pseudomonas delafieldii* have previously been used in such a process to desulfurize a model oil (Li et al. 2009). When compared to freely suspended cultures, both types (immobilized and free) showed similar desulfurizing activity during the first batch cycle. However, the immobilized cells could be reused for up to seven batch cycles while retaining 80% of their specific desulfurizing activity. Free cells only retained 15% of their specific desulfurizing activity after one use (Li et al. 2009). Therefore, the hypothesis of this work was that successful immobilization of the anaerobic dark fermentation organism *Clostridium beijerinckii* will reduce the lag growth phase between dark fermentation batches. The volume of hydrogen produced will thus be higher over a given time period compared to a freely suspended culture. Therefore, overall volumetric hydrogen production will increase

compared to a non-immobilized system over repeated batch cycles. One batch cycle is defined as the time from fresh media addition to spent liquid removal. Such a process has not yet been designed for hydrogen production, and thus this novel research may help to reduce the current economical barrier to entry for industrial biohydrogen production.

Materials and Methods

Chitosan (low molecular weight, 75-85% deacetylated), NaCl and magnetite nanoparticles (nano powder, <50nm) were purchased from Sigma-Aldrich (Oakville, ON, Canada). Glacial acetic acid and NaOH were purchased from Fisher Scientific (Ottawa, ON, Canada). Alginic acid (low viscosity) was purchased from MP Biomedicals (Solon, OH, United States).

Bare magnetite NPs were functionalized prior to immobilization using a layer-by-layer (LbL) technique in order to enhance growth of the bacteria on the surface of the particles. The outermost layer must possess traits to promote bacterial attachment such as biocompatibility, electrostatic or hydrophobic characteristics or induce nano-size effects when interacting with the bacterial cell wall.

This LbL method relies on electrostatic interactions between the core nanoparticles and each subsequent polyelectrolyte layer of opposite charge. Thus, a negatively charged core nanoparticles is first coated with a cationic polyelectrolyte, inverting the overall surface charge. An anionic polyelectrolyte can then be deposited as a second layer, again inverting the overall surface charge. This process is repeated for any number of layers whereby the final surface characteristics of the NP-polyelectrolyte hybrid are determined by the final layer (Decher 1997; Masereel et al. 2011). Appropriate polyelectrolytes must be chosen when working with biological samples. Primarily, the layer materials must be biocompatible and non-toxic; two common characteristics of many biopolymers. Thus, the procedure used here consisted in

depositing chitosan (cationic polyelectrolyte) onto the magnetite NP surface followed by alginic acid (anionic polyelectrolyte) as shown in **Error! Reference source not found.**. Chitosan is a polyaminosaccharide composed of repeating glucosamine units. Thus, it contains amino groups providing a cationic charge (Pillai et al. 2009). Conversely, alginic acid is composed of α-L-guluronate and β-D-mannuronate units with carboxyl functional groups providing a net anionic charge (Ye et al. 2005). This alginic acid layer is expected to provide the desired conditions discussed above for bacterial attachment to the particle surface. A 2g/L chitosan solution was prepared in 2% acetic acid containing 0.01M NaCl (prepared in reverse osmosis (RO) water). This solution was filtered using P8 filter paper and degassed for 20 minutes in a Branson 2510 sonicating bath. Dry magnetite NPs were added to the chitosan solution under sonicating to a final concentration of 0.1g/L magnetite. This solution was sonicated for 1 hour, shaking by hand every 15 minutes. NPs were washed twice with RO water (pH 3) by centrifugation at 10000 rpm for 20 minutes followed by re-suspension in RO water (pH 3). After 2 wash cycles, the particles were again centrifuged at 10000 rpm for 20 minutes before being re-suspended in RO water (pH 3). Chitosan coated NPs (C-NPs) were then coated with alginic acid (A-C-NPs) according to the same procedure, except all aqueous solutions were set to pH 7 with NaOH.

Confirming coatings and preparing for immobilization

The presence of chitosan and alginic acid coatings were confirmed through zeta potential measurements and TEM images. The zeta potential of bare magnetite nanoparticles, C-NPs and A-C-NPs were determined using a Malvern Zetasizer Nano ZS90. TEM images were obtained using a Philips CM200 200kV TEM. Even though C-NPs would in theory have a greater electrostatic interaction with a negatively charged bacterial cell well, C-NPs poor solubility in neutral solutions, resulted in agglomeration, reducing the overall surface area available for

immobilization. Therefore, only A-C-NPs were used for immobilization studies. Prior to use in the biohydrogen production experiments, A-C-NPs were transferred to 100ml serum bottles sparged with argon gas to remove all dissolved oxygen, sealed with butyl rubber stoppers and capped with aluminum crimps before being autoclaved at 121°C for 30 minutes and cooled down for later addition to test bottles.

Immobilizing *Clostridium beijerinckii* (NCIMB8052) and hydrogen production experiments at the 100ml scale

Clostridium beijerinckii (NCIMB 8052) were inoculated into 100ml culture bottles containing 50ml of oxygen free 2xTY media (5g/L glucose as a carbon source) and grown to mid-log phase at 35ºC and 100rpm. 2xTY media was chosen as tryptone contains nitrogen sources and amino acids required for bacterial growth while yeast extract acts as an adequate vitamin source. Autoclaved A-C-NPs prepared previously were then added to the growing 100ml culture bottle to a final concentration of 0.25g/L and incubated for 6 hours. This initial incubation, known as the pre-culture preparation, was meant to allow exponentially growing bacteria to interact with the A-C-NPs and complete the immobilization process. After this time period, a permanent magnet was applied to the culture bottle to separate the nanoparticles and immobilized biomass from the liquid media. The liquid phase was removed and 4ml of anaerobic Phosphate Buffered Saline (PBS) buffer were added as a washing step. A permanent magnet was again applied to the culture bottle, separating the nanoparticles and immobilized biomass from the PBS buffer. The buffer was then removed and 30ml of fresh 2xTY media with 5g/L glucose was added in order to start the biohydrogen production experiment.

Total gas production was measured every two hours over the sampling period of up to 24 hours and analyzed for hydrogen concentration (see analytical methods section). Biomass growth

was measured at specific time intervals via optical density measurements (see analytical methods section). After approximately 24h of growth, a permanent magnet was again applied to the culture bottle, separating the immobilized biomass from the liquid media and non-immobilized bacteria. This spent liquid and non-immobilized bacterium was then removed and 30ml of fresh 2xTY media with 5g/L glucose was added to begin the second fermentation cycle. After approximately 17h of growth, this cycling process was repeated for a third fermentation cycle of approximately 12.5h in length. All trials were performed in duplicate. Controls consisted of test bottles without nanoparticles. Cycling time periods were allowed to continue until the stationary growth phase was reached.

Scale-up of biohydrogen production

In order to further evaluate the effects of immobilization *C. beijerinckii* on the prepared NPs, scale-up trials involving 100 ml, 250 ml and 3.6 L batch reactors were performed. The fermentation and cycling procedure was identical to that described for the immobilization trials with slight differences. 100 ml trials were performed exactly as described in the initial immobilization studies without the PBS washing step. The 250 ml reactors consisted of 250 ml Wheaton bottles with screw caps containing grey butyl rubber septa. 3.6L batch trials were performed in a 3.6L Infors HT Labfors 4 bioreactor with X-DDC operating panel. This reactor was also supplied with 10% (w/v) NaOH to maintain reactor pH at 7.0 and a 1% (v/v) solution of Antifoam A to prevent foaming. A water circulating jacket was used to maintain temperature control at 35°C within the reactor and agitation was applied via a dual impeller at 500 rpm. The 3.6 L reactor trials represent preliminary scale-up as only one trial was performed.

The A-C-NP concentration was also increased in an effort to achieve a greater amount of immobilized biomass and in accordance with NP concentrations used in literature (Ghosh et al.

2011; Ghosh et al. 2010a; Ghosh et al. 2010b). Cycling time periods were decreased to a maximum of 13h to prevent stationary phase cell death from influencing the activity of immobilized bacteria. The only exception to this rule came if biomass growth in all samples had not reached late exponential phase by 13h. Finally, a greater volume of fresh media was used to initiate each cycle. Differences in reactor operational parameters are outlined in **Error! Reference source not found.**. Initial and cycled media volumes refer to the amount of fresh 2xTY media used for initial immobilization (prior to cycle 1) and 2xTY media added following each cycling period, respectively.

Analytical methods

Total gas production was measured using a frictionless syringe, every 2 hours during the immobilization studies and every 3-10h during the scale up study. Hydrogen concentration in the biogas produced was analyzed using a Hewlett Packard GC model 5890 gas chromatograph equipped with a 6A molecular sieve column and a thermal conductivity detector (TCD). The column temperature was maintained at 80°C, injection temperature at 100°C and TCD at 100°C with 2.0 ml/min Argon as a carrier gas. 2ml gas samples were collected from the reactor using a gas-tight Hamilton 2ml syringe for injection into the GC. Biomass production was also measured every 3-10h via optical density measurements. The permanent magnet was first placed against the side of the reactor to separate immobilized biomass from the bulk solution. From this bulk solution, 1ml samples were extracted and measured at 600nm with Ocean Optics CHEMUSB4-UV-VIS spectrophotometer, (200-850 nm). Substrate consumption during initial immobilization trials was analyzed using the Glucose GO Assay kit from Sigma-Aldrich (Oakville, ON, Canada), following the manufacturer's experimental procedure.

During scale up trials, glucose and fermentation metabolite concentrations were also analyzed by High Performance Liquid Chromatography (HPLC). An HP model 1050 HPLC equipped with a Resex ROA Organic Acid H+ 8% 150x7.8mm column was used to measure concentrations of pyruvate, lactate, formate, acetate, butyrate, ethanol and glucose. The mobile phase used was 0.035M H_2SO_4 at a flow rate of 0.8ml/min and run time of 12 minutes. The column temperature was maintained at 35°C. UV and refractive index (RI) detectors were used to quantify organic acids and alcohols, respectively. The RI detector was used to measure glucose composition in each sample. The UV detector was operated at 195nm while the RI detector was maintained at 35°C.

Results

Nanoparticles coating confirmation

The zeta potential (ζ) of bare NPs, C-NPs and A-C-NPs were determined to verify the presence of each coating. Chitosan carries a characteristic positive charge, while alginic acid induces an anionic surface charge. All values are based on a six zeta potential readings and averages are outlined in **Error! Reference source not found.**. Errors represent standard deviations between repeated readings. The zeta potentials of coated particles were also measured following autoclaving to determine the effect of sterilization on the coatings. Comparison of the zeta potential before and after autoclaving indicated some coating loss; between 12-23% of the change in zeta-potential being lost.

TEM images were also analyzed to visualize each layer and ensure coated particles remained below 100 nm in diameter. **Error! Reference source not found.** displays these results for autoclaved samples, which confirm the nanoparticles size remained below 100 nm and show the presence of each coating. Further, the white arrows in **Error! Reference source not found.**b

and 1c indicate the presence of chitosan and chitosan-alginic acid layers, respectively. Therefore, the layer-by-layer method successfully functionalized the magnetite NPs, preparing them for bacterial immobilization.

Bacterial immobilization confirmation

Initial trials in the 100 ml reactor indicated increased gas production and a shorter lag growth phase with A-C-NPs compared to controls but only for the second immobilization cycle, as depicted in **Error! Reference source not found.**a and 2b. There were no large differences in hydrogen production between the A-C-NP samples and control during the first and third cycles. However, during the second cycle, A-C-NP samples produced a minimum of 102% more hydrogen than the control. These results, particularly the shorter lag growth phase, indicated more biomass was retained within the A-C-NP reactors than controls. To confirm this retention was due to the attachment of NPs to the bacterial cell wall, samples incubated with NPs during the pre-culture step were imaged as shown in **Error! Reference source not found.** to confirm initial cell-NP immobilization. A second sample consisting of bacteria which had been cycled once are imaged in **Error! Reference source not found.**b to confirm the cycling process did not reverse the immobilization procedure or strip NPs from the cell wall. Although **Error! Reference source not found.**a suggests possible NP agglomeration occurring during the pre-culture stage, it does confirm the immobilization procedure was successful in attaching A-C-NPs to bacterial cell walls.

Fermentation results

Over the course of three fermentation cycles, the 100ml reactors produced 85.1 ml of hydrogen as depicted in **Error! Reference source not found.**a. This equates to a volumetric production of 14.2 (±1.5) ml-H_2/L/h and molar production of 0.6 (±0.1) mmol/L/h. Utilizing the established

HPLC method described under the analytical methods section, the only liquid metabolites produced in measureable quantities were ethanol, acetate and formate, shown in **Error! Reference source not found.**. The patterns of production were similar from one cycle to another, with glucose conversion in the 15.7-32.4% range, ethanol and acetate produced in comparable amounts and a lower production of formate (about three times less than the other metabolites).

The 250 ml reactors experienced a significant loss of immobilized biomass during the cycling process, which resulted in large errors in hydrogen production and biomass growth during cycle two. This loss was due to limited ability to retain the NPs using the magnets available at that time. Due to such a large loss of A-C-NPs, this scale of reactors was only cycled twice. All other reactors were cycled three times and bigger magnets were used for the 3.6 L reactor. The resulting total hydrogen, ethanol, acetate and formate production across all cycles of each reactor are presented in **Error! Reference source not found.** for scale up comparison. Based on **Error! Reference source not found.**, the 250ml reactor resulted in a volumetric hydrogen production of 77.6 (±33.4) ml/L/h (comparable to the value of 85.1 ml/L/h obtained in the immobilization study) and molar production of 3.2 (±1.4) mmol/L/h.

The 3.6 L dataset are preliminary in nature however this initial trials resulted in a volumetric hydrogen production of 37.6 ml/L/h and molar production of 1.6 mmol/L/h. The relative production profiles of all metabolites were similar across all scales (ethanol and acetate representing the primary and secondary metabolites respectively), except for formate at the largest scale. The 3.6 L reactor dataset suggest a shift in metabolic processes at this larger scale as no formate was produced in measureable quantities.

Process efficiencies

Substrate conversion efficiency (SCE), energy conversion efficiency (ECE) and specific hydrogen productivity (SHP) were determined to evaluate the overall performance of the hydrogen production process. SCE was calculated based on the complete theoretical conversion of glucose to hydrogen, yielding 4 moles of hydrogen for every 1 mole of glucose consumed (Levin et al. 2004). Therefore, the SCE was calculated according to Equation 1:

$$\boldsymbol{SCE} = \frac{\boldsymbol{mol}_{\boldsymbol{H_2\ produced}}}{\boldsymbol{mol}_{\boldsymbol{glucose\ added}}} \cdot \frac{\boldsymbol{1\ mol\ glucose}}{\boldsymbol{4\ mol H_2}} \cdot \boldsymbol{100\%} \qquad \text{(Equation 1)}$$

The amount of hydrogen produced was converted from volume to moles assuming hydrogen acted as an ideal gas. The pressure was assumed to be atmospheric (1 atm) and at room temperature in the lab (21°C). The ECE was calculated comparing the total specific energy of glucose added to the system to the total specific energy of hydrogen produced. The specific energy (or energy density) of hydrogen is 142 kJ/g (Ghosh and Hallenbeck 2014), while that of glucose is 16 kJ/g (Kraisid 2003). Therefore, the ECE is given by Equation 2:

$$\boldsymbol{ECE} = \frac{\boldsymbol{m_{H_2} \cdot E_{H_2}}}{\boldsymbol{m_{glucose} \cdot E_{glucose}}} \cdot \boldsymbol{100\%} \qquad \text{(Equation 2)}$$

m_x represents the mass of hydrogen produced or glucose added in grams, while E_x represents the specific energy of the corresponding component.

The SHP based on biomass growth was determined from the ratio of hydrogen produced to maximum biomass reading according to Equation 3:

$$\boldsymbol{SHP} = \frac{\boldsymbol{mmol}_{\boldsymbol{H_2\ produced}}}{\boldsymbol{OD600}} \qquad \text{(Equation 3)}$$

Error! Reference source not found. depicts the efficiencies and specific productivity calculated for each reactor size. This data indicates an initial increase in efficiency when scaling up to the

250ml reactors, followed by a large decrease when scaled up further to the 3.6 L reactor. The exception to this trend was the specific hydrogen productivity normalized against biomass optical density reading which significantly increased at the highest reactor scale. Large changes in optical density measurements were not expected from scale to scale, however the amount of hydrogen produced was expected to vary directly with reactor size, which might explain this result. In order to facilitate comparison of substrate conversion efficiencies to previously published data, the SCEs calculated above are presented in **Error! Reference source not found.** as the equivalent molar yield of hydrogen ($Y_{H2/S}$; mol-H_2/mol-glucose). All of the hydrogen yields ($Y_{H2/S}$) obtained in the present study lie within the range of data previously published by Rittmann and Herwig (Rittmann and Herwig 2012).

Volumetric hydrogen production

Based on the results presented above, the addition of A-C-NPs resulted in greater biomass retention between cycles and a shortened lag phase (data not shown for the 250 ml and 3.6 L reactors), which thus resulted in a greater overall gas production. This indicates that optimizing cycling conditions and techniques might further enhance the effect of A-C-NPs. The greater hydrogen production obtained in the second fermentation cycle of the 100 ml reactors was likely due to an acclimation period during the first cycle and a loss of immobilized biomass leading to the third cycle. This hypothesis is supported by comparison of the results obtained at each scale. For the 100 ml reactor, hydrogen production increased by 102% but overall there was not a measureable difference in hydrogen production between the A-C-NP reactors and controls over the course of all three cycles. For the 250 ml reactors, again cycle two did not produce a noticeable difference in hydrogen production compared to the control, likely due to a significant loss in immobilized biomass resulting from an insufficient retention procedure. However, at this

scale the initial acclimation was not experienced as much compared to the 100 ml trials. The first cycle resulted in a 280% increase in hydrogen production compared to the controls. This result indicates the acclimation period of the 100 ml trials may have resulted from a small total initial population, not experienced at larger scale. For the 3.6 L reactor, again the acclimation period exhibited in the 100 ml reactor was not observed, supporting the hypothesis that the adjustment period in the 100 ml reactor was due to a small total bacterial population at the smaller scale. Further, the 3.6 L reactor produced greater hydrogen than the control over all three cycles. The overall process resulted in a 98% increase in hydrogen production compared to the control. Overall, the proposed immobilizing and cycling procedure was to some extent successfully applied across all reactor sizes. However, there is still room for improvement in order to achieve greater hydrogen production in a sustainable manner.

Conversion efficiencies and productivity

The overall SCE increased during scale-up to 250 ml but decreased significantly when scaled up to 3.6 L. This may be due to changes in metabolic pathways whereby the concentration of hydrogen in the gas stream of the 3.6 L reactor decreased compared to the smaller scales. The large decrease in SCE was not accompanied by a corresponding increase in the other metabolites detected. In evaluating the specific trends in metabolite production, ethanol concentrations remained relatively constant between scales while acetate and formate concentrations decreased in the 3.6 L reactor. One hypothesis would suggest the differences were spread among numerous other metabolites which were not produced in measureable quantities. Such metabolites include lactate, propionate, acetaldehyde and butyrate. The formation of butyrate would have a compounding effect as it also would have resulted in higher CO_2 production (Levin et al. 2004). This is reflected in the hydrogen concentration of the reactor head spaces which ranged from

27%-45% in the 100ml reactors, 27%-74% in the 250 ml reactors and only 20%-37% in the 3.6 L reactor. The fact butyrate was not produced in greater quantities is likely due to the primary production of ethanol competing with the butyric acid pathway (Lee et al. 2008).

The production of acetate during fermentation is an unavoidable by-product of hydrogen production and it is only produced under the regeneration of ATP (cellular energy) which can be used to further produce biomass (and thus indirectly produce hydrogen) as shown in **Error! Reference source not found.**. Therefore the presence of acetate is not intolerable. Ethanol, however, is a by-product of a metabolic pathway that not only terminates without additional hydrogen production, but produces metabolites which compete with hydrogen producing reactions. This pathway utilizes 1 mole of NADH to produce acetaldehyde and 1 mole of NAD^+. Acetaldehyde is then further metabolized using 1 mole of NADH to produce ethanol and 1 mole of NAD^+. Therefore, every time ethanol is produced, at least 2 moles of NAD^+ are released. NAD^+ can then be recycled back to NADH in a reaction competing with hydrogen production (Lee et al. 2008). It is thus clear that the high presence of ethanol indicates the organisms are not efficiently producing hydrogen. The fact ethanol is the primary metabolite produced over all three reactor scales also indicates there is significant room for improving process efficiency on a cellular level.

ECE remained relatively unchanged between the 100 ml and 250 ml reactors; however it decreased greatly when scaling up to the 3.6 L reactor. Again, this was likely due to the changes in metabolic pathways. The SHP steadily increased with each scale-up as expected. The maximum optical density between different sized reactors did not change significantly, however the total amount of hydrogen produced changed in proportion to reactor size. Perhaps the most intriguing difference was the changes in molar hydrogen yield between scales. Hydrogen yield

increased by nearly a factor of 2.5 from the 100 ml reactors to the 250 ml reactors, but then decreased by a factor of almost 4.9 when scaled up to the 3.6 L reactor. This indicates unwanted side reactions or metabolic pathways taking place within the 3.6 L reactor. This discrepancy may be due to large changes in environmental conditions such as type of agitation (stirred incubator vs. impeller), pH (decreasing vs. constant), antifoaming agent (not-present vs. present), oxygen partial pressure (pO_2) control (small volume vs. large volume) (Bartacek et al. 2007) and overall changes in process techniques as described in the Scale-up of biohydrogen production previous section. Further, the overall poor hydrogen productivity of all three reactor sizes when compared to those in literature may be attributed to NP stripping. This term refers to both NPs being stripped from the cell wall after initial attachment or the stripping of the polyelectrolyte coatings during the fermentation process. TEM images indicated A-C-NPs weren't striped from the cell wall after one cycle, but this attachment may degrade over prolonged time periods or under different conditions experienced in varying reactor sizes. Although the hydrogen yields produced lie within the range of data assembled (Rittmann and Herwig 2012), the values presented here do not exceed previously published results, as shown in **Error! Reference source not found.**. Therefore, incorporating the manufactured nanoparticles into a biohydrogen process requires further enhancement in order to justify the increased capital and operational costs associated with this approach.

Discussion

The major objective of this study was to ameliorate hydrogen production using *Clostridium beijerinckii* Immobilized with chitosan-alginic acid polyelectrolytes functionalized magnetite nanoparticles. The production of biohydrogen from difference carbon sources has been studied extensively in *Clostridium* sp. (Ghosh and Hallenbeck 2014), but immobilization studies were

not carried out in details concerning suitability of immobilizing materials, molecular interactions between immobilizing materials towards microorganisms and industrial feasibility. Several materials were applied to immobilize the *Clostridium* sp. time to time to improve hydrogen production. Polyethylene glycol (PEG) gel was fabricated and used as a carrier to immobilize *Clostridium* sp. LS2 for continuous hydrogen production (Singh et al. 2013). *Clostridium* sp. T2 cells were immobilized by entrapment into calcium alginate beads (Zhao et al. 2013). Hydrogen producing anaerobe, *C. tyrobutyricum* JM1 was immobilized using polyurethane foam as support (Jo et al. 2008) toward improving hydrogen production. polyurethane-activated carbon matrix were also used as a immobilizing substance for *Clostridium tyrobutyricum* ATCC 25755 (Mitchell et al. 2009). *Clostridium butyricum* was immobilized in a porous carrier (acetyl cellulose filter) with agar for hydrogen production to see the effect of vitamine and nitrogen source upon hydrogen production (Karube et al. 1982). Though hydrogen yield and productivity were improved using PEG, algenate bead, polyurethane foam, polyurethane-activated carbon matrix upon pure substrates or industrial wastes, but major issue still remains about the reusability, stability and regeneration of immobilizing materials. In a recent studies it has also been emphasized that free energy change is another vital factor when *Clostridium* sp. CFPA-20 isolate adheres to polyethylene glycol-b-polypropylene glycol immobilizing material. the alterations in free energy upon molecular interaction of adhesion to polymeric resin and self-agglomeration were both negative, indication that *Clostridium* sp. CFPA-20 was thermodynamically favored for immobilization (Nomura et al. 2014). Based on this current scenario, Bare magnetite nanoparticles were successfully coated with chitosan and alginic acid layers before attachment to *C. beijerinckii* cultures for the first time. This immobilization technique enabled the retention of biomass within bioreactors of varying sizes

and use in successive batch fermentations for hydrogen production. This process has the advantages of reducing downtime between batches and increasing the volumetric production of hydrogen over a given time period. Although efficiency and processing issues presented themselves, it was shown that an external magnetic field could retain the immobilized biomass within the reactor, producing greater amounts of hydrogen than a control reactor in the same time period. However, the low substrate and energy conversion efficiencies compared to previously published data indicate that there is room for significant improvement. Another major concern for improving hydrogen production is the metabolic carbon flow and reduced equivalent regeneration and utilization (e.g. NADH, NAD[P]H). NADH regeneration and utilization has predominantly been dominated by ethanol, lactate, Butanol metabolic networks which are indirectly competing with hydrogen generation involving PFOR and NFOR pathways in Fig. S1. It has been evident that regeneration of reduced equivalents by Immobilized whole cells of *Clostridium butyricum* is feasible but only bottleneck is hydrogen partial pressure (Matsunaga et al. 1985) In this current study, ethanol and acetate are most predominant end metabolites during hydrogen production. Ethanol is produced over all three scale reactors indicating space for improving the hydrogen yield by knocking out those competing metabolic pathways. Thus far metabolically engineering in *Clostridium beijerinckii* followed by immobilization of those mutant strains on chitosan-alginic acid polyelectrolytes functionalized magnetite nanoparticles, could be the best future option for enhancing substrate and energy conversion efficiencies upon hydrogen production. Whereas, production of acetate is completely unavoidable due to its relatedness with ATP regeneration for cellular energy supply. Further, the decrease in some process efficiencies during scale up from 250 ml to 3.6 L reactors indicates environmental factors such as agitation, pH, antifoaming and pO_2 must be optimized in

order to maximize hydrogen yields at larger scales. Future research should also consider optimization of media components or reactor conditions to promote greater hydrogen production from a metabolic standpoint while suppressing ethanol formation. Finally, a more uniform or stronger magnetic retention mechanism may be developed in order to retain a greater amount of immobilized biomass during batch cycling. Although this process is not yet ready for large scale biohydrogen production, this study demonstrated that coated NPs can be attached to biohydrogen producing organisms and used as a retention mechanism for increasing volumetric hydrogen production.

Acknowledgements

We would like to thank Prof. Patrick C. Hallenbeck for his suggestion time to time. Special thanks to Mr. Ranjan Roy for his help with analytical equipment and Dr. David Liu for his help with TEM imaging. Funding for this research was provided by FRQNT - Project de recherché en équipe. T. Seelert and D. Ghosh were supported by a Eugenie Ulmer Lamothe and FQRNT-PBEEE Scholarships, respectively.

References

Bartacek J, Zabranska J, Lens PNL (2007) Developments and constraints in fermentative hydrogen production. Biofuels, Bioprod Biorefin 1(3): 201-214. doi: 10.1002/bbb.17

Brentner LB, Peccia J, Zimmerman JB (2010) Challenges in Developing Biohydrogen as a Sustainable Energy Source: Implications for a Research Agenda. Environ Sci Technol 44(7): 2243-2254. doi: 10.1021/es9030613

Chen X, Sun Y, Xiu Z, Li X (2006) Zhang D Stochiometric analysis of biological Hydrogen production by fermentative bacteria. Int J Hydrogen Energy 31(4): 539-549. doi.org/10.1016/j.ijhydene.2005.03.013

Conti J, Holtberg P (2011) International Energy Outlook U.S.E.I. Administration, Washington, DC.DOE/EIA-0484(2011). http://large.stanford.edu/courses/2012/ph241 /miller1/docs/0484-2011.pdf. Accessed September 2011

Cranston GR, Hammond GP (2010) North and south: Regional footprints on the transition pathway towards a low carbon, global economy. Appl Energ 87(9): 2945-2951. doi:10.1016/j.apenergy.2009.08.015

Cullen JM, Allwood JM (2010) The efficient use of energy: Tracing the global flow of energy from fuel to service. Energ Policy 38: 75-81. doi:10.1016/j.enpol.2009.08.054

Decher G (1997) Fuzzy Nanoassemblies: Toward Layered Polymeric Multicomposites. Science 277(5330): 1232-1237. doi:10.1126/science.277.5330.1232

Ghosh D, Hallenbeck PC (2014) Metabolic Engineering: Key for Improving Biological Hydrogen Production. In. Lu X (ed) Biofuels from Microbes to Molecules, 1st edn. Horizon Scientific Press, United Kingdom, pp 1-46

Ghosh D, Pramanik A, Sikdar N, Ghosh SK, Pramanik P (2010) Amelioration Studies on Optimization of Low Molecular Weight Chitosan Nanoparticle Preparation, Characterization With Potassium Per Sulphate and Silver Nitrate Combined Action With Aid of Drug Delivery to Tetracycline Resistant Bacteria. Int J Pharm Sci Drug Res 2(4): 247-253

Ghosh D, Pramanik P (2010) Low Molecular Weight Biodegradable Polymer Based Nanoparticles as Potential Delivery Systems for Therapeutics: The Way Forward? Int J Pharm Sci Drug Res. 2(1): 31-34

Ghosh D, Pramanik A, Sikdar N, Pramanik P (2011) Synthesis of low molecular weight alginic acid nanoparticles through persulfate treatment as effective drug delivery system to manage drug resistant bacteria. Biotechnol Bioprocess Eng 16(2): 383-392. doi: 10.1007/s12257-010-0099-7

Hallenbeck PC, Ghosh D (2009) Fermentative hydrogen production: the way forward? Trends Biotechnol 27: 287-297. doi: 10.1016/j.tibtech.2009.02.004

Hayashi M, Hughes L (2013) The Fukushima nuclear accident and its effect on global energy security. Energ Policy 59: 102-111. doi:10.1016/j.enpol.2012.11.046

Jo JH, Lee DS, Park D, Park JM (2008) Biological hydrogen production by immobilized cells of *Clostridium tyrobutyricum* JM1 isolated from a food waste treatment process. Bioresour Technol 99(14): 6666-6672. doi: 10.1016/j.biortech.2007.11.067

Karube I, Urano N, Matsunaga T, Suzuki S (1982) Hydrogen Production from Glucose by Immobilized Growing Cells of *Clostridium butyricum*. Eur J Appl Microbiol Biotechnol 16:5-9. doi: 10.1007/BF01008235

Koskinen PE, Beck SR, Orlygsson J, Puhakka JA (2008) Ethanol and hydrogen production by two thermophilic, anaerobic bacteria isolated from Icelandic geothermal areas. Biotechnol Bioeng 101(4): 679-690. doi: 10.1002/bit.21942

Kothari R, Tyagi VV, Pathak A (2010) Waste-to-energy: A way from renewable energy sources to sustainable development. Renew Sust Energ Rev 14(9): 3164-3170. doi: 10.1016/j.rser.2010.05.005

Kraisid, T (2003) Rome: Food and Agriculture Organization of the United Nations, Rome, (2003). http://www.fao.org/uploads/media/FAO_2003_Food_Energy_02.pdf. Accessed December 2003

Lee H-S, Salerno MB, Rittmann BE (2008) Thermodynamic Evaluation on H_2 Production in Glucose Fermentation. Environ Sci Technol 42(7): 2401-2407. doi: 10.1021/es702610v

Levin DB, Pitt L, Love M (2004) Biohydrogen production: prospects and limitations to practical application. Int J Hydrogen Energy 29(2): 173-185. doi: 10.1016/S0360-3199(03)00094-6

Li YG, Gao HS, Li WL, Xing JM, Liu HZ (2009) *In situ* magnetic separation and immobilization of dibenzothiophene-desulfurizing bacteria. Bioresource Technol 100(21): 5092-5096. doi:10.1016/j.biortech.2009.05.064

Lin CN, Wu SY, Chang JS, (2006) Fermentative hydrogen production with a draft tube fluidized bed reactor containing silicone-gel-immobilized anaerobic sludge. Int J Hydrogen Energy 31(15): 2200-2210. doi:10.1016/j.ijhydene.2006.05.012

Lin CN, Wu SY, Chang JS, Chang JS (2009) Biohydrogen production in a three-phase fluidized bed bioreactor using sewage sludge immobilized by ethylene–vinyl acetate copolymer. Bioresource Technol 100(13): 3298-3301. doi: 10.1016/j.biortech.2009.02.027

Masereel B, Dinguizli M, Bouzin C, Moniotte N, Feron O, Gallez B, Borght TV, Michiels C, Lucas S (2011) Antibody immobilization on gold nanoparticles coated layer-by-layer with polyelectrolytes. J Nanopart Res 13(4): 1573-1580. doi:10.1007/s11051-010-9908-3

Masset J, Calusinska M, Hamilton C, Hiligsmann S, Joris B, Wilmore A, Thornart P (2012) Fermentative hydrogen production from glucose and starch using pure strains and artificial co-cultures of *Clostridium* spp. Biotechnol Biofuel 5:35. doi:10.1186/1754-6834-5-35

Matsunaga T, Matsunaga N, Nishimura S (1985) Regeneration of NAD(P)H by immobilized whole cells of *Clostridium butyricum* under hydrogen high pressure. Biotechnol Bioeng 27(9):1277-1281. doi: 10.1002/bit.260270902

Mitchell RJ, Kim J-S, Jeon B-S, Sang B-I (2009) Continuous hydrogen and butyric acid fermentation by immobilized *Clostridium tyrobutyricum* ATCC 25755: Effects of the glucose concentration and hydraulic retention time. Bioresour Technol 100: 5352–5355. doi: 10.1016/j.biortech.2009.05.046

Nomura T, Naimen A, Toyoda S, Kuriyama Y, Tokumoto H, Konishi Y (2014) Isolation and characterization of a novel hydrogen-producing strain *Clostridium* sp. suitable for immobilization. Int J Hydrogen Energ 39: 1280-1287. doi: 10.1016/j.ijhydene.2013.10.166

Pan C-M, Fan Y-T, Zhao P, Hou H-W (2008) Fermentative hydrogen production by the newly isolated *Clostridium beijerinckii* Fanp3. Int J Hydrogen Energy 33(20): 5383-5391. doi:10.1016/j.ijhydene.2008.05.037

Pielke R, Wigley T, Green C (2008) Dangerous assumptions. Nature 452(7187): 531-532. doi:10.1038/452531a

Pillai CKS, Paul W, Sharma C (2009) Chitin and chitosan polymers: Chemistry, solubility and fiber formation. Prog Polym Sci 34(7): 641-678. doi:10.1016/j.progpolymsci.2009.04.001

Rittmann S, Herwig C (2012) A comprehensive and quantitative review of dark fermentative biohydrogen production. Microb Cell Fact 11:115. doi:10.1186/1475-2859-11-115

Singh L, Siddiqui MF, Ahmad A, Rahima MHA, Sakinah, Wahid ZA (2013) Application of polyethylene glycol immobilized *Clostridium* sp. LS2 for continuous hydrogen production from

palm oil mill effluent in up flow anaerobic sludge blanket reactor. Biochem. Eng. J. Biochemical Engineering Journal 70: 158–165. doi:10.1016/j.bej.2012.10.010

Taguchi F, Mizukami N, Hasegawa K, Saito-Taki T (1994) Microbial conversion of arabinose and xylose to hydrogen by a newly isolated *Clostridium* sp. No. 2. Can J Microbiol 40(3): 228-233. doi:10.1139/m94-037

Wang X, Hoefel D, Saint CP, Monis PT, Jin B (2007) The isolation and microbial community analysis of hydrogen producing bacteria from activated sludge. J Appl Microbiol 103(5): 1415-1423. doi: 10.1111/j.1365-2672.2007.03370.x

Ye S, Wang C, Liu X, Tong Z (2005) Multilayer nanocapsules of polysaccharide chitosan and alginate through layer-by-layer assembly directly on PS nanoparticles for release. J Biomater Sci, Polym Ed 16(7): 909-923. doi: 10.1163/1568562054255691

Zhao L, Cao G-L, Wang A-J, Guo W-Q, Liu B-F, Rena H-Y, Rena N-Q, Ma F (2012) Enhanced bio-hydrogen production by immobilized *Clostridium* sp. T2 on a new biological carrier. Int J Hydrogen Energ 37: 162-166. doi: 10.1016/j.ijhydene.2011.09.103

Zhao X, Xing D, Fu N, Liu B, Ren N (2011) Hydrogen production by the newly isolated *Clostridium beijerinckii* RZF-1108. Bioresource Technol 102(18): 8432-8436. doi: 10.1016/j.biortech.2011.02.086

Fig.S1

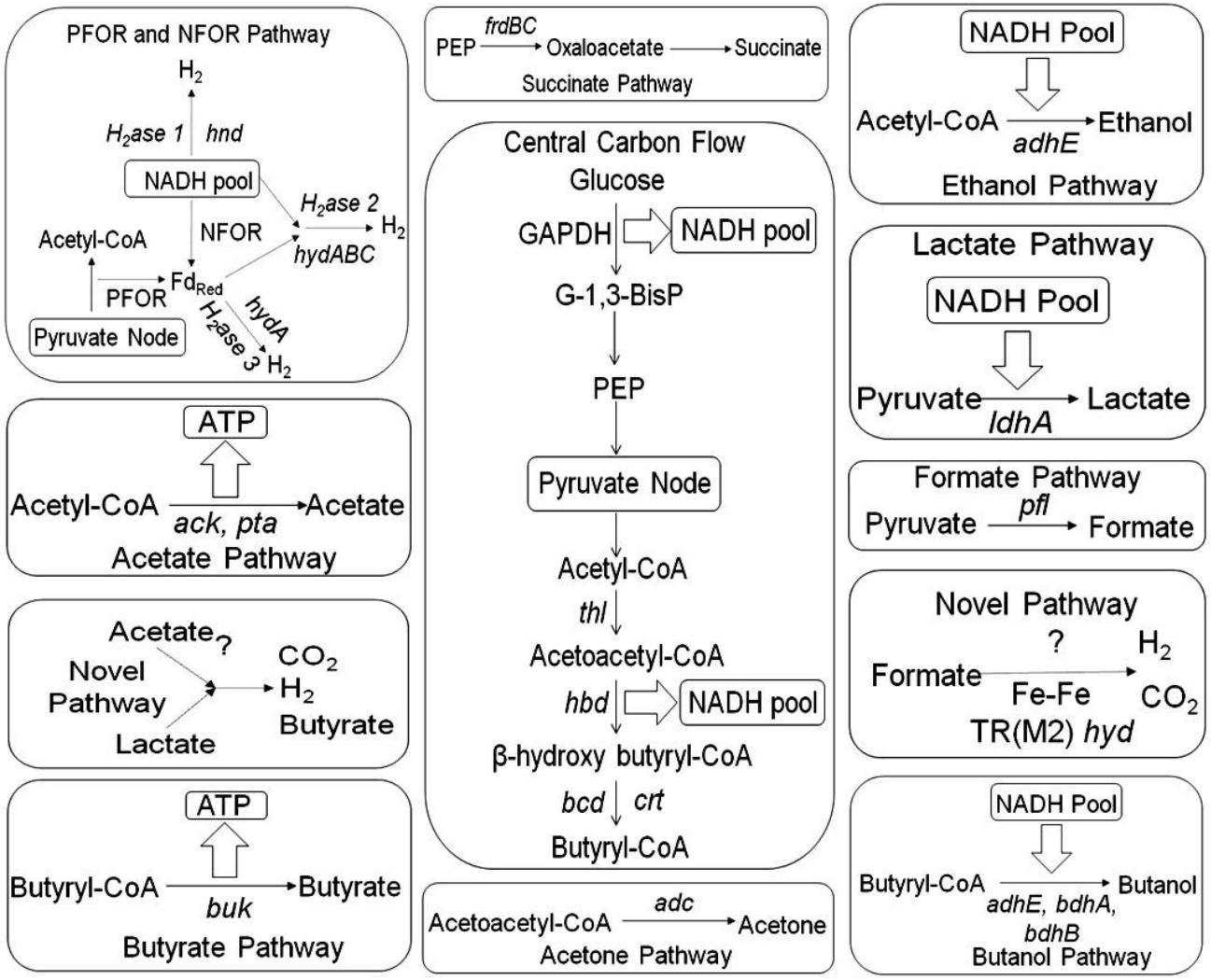
PFOR and NFOR Pathway
H_2
H_2ase 1
hnd
NADH pool
H_2ase 2
H_2
Acetyl-CoA
NFOR
hydABC
PFOR
Fd_{Red}
hydA
Pyruvate Node
H_2ase 3
H_2
ATP
Acetyl-CoA
Acetate
ack, pta
Acetate Pathway
Acetate
?
Novel Pathway
CO_2
H_2
Butyrate
Lactate
ATP
Butyryl-CoA
Butyrate
buk
Butyrate Pathway
frdBC
PEP
Oxaloacetate
Succinate
Succinate Pathway
Central Carbon Flow
Glucose
GAPDH
NADH pool
G-1,3-BisP
PEP
Pyruvate Node
Acetyl-CoA
thl
Acetoacetyl-CoA
hbd
NADH pool
β-hydroxy butyryl-CoA
bcd
crt
Butyryl-CoA
Acetoacetyl-CoA
adc
Acetone
Acetone Pathway
NADH Pool
Acetyl-CoA
Ethanol
adhE
Ethanol Pathway
Lactate Pathway
NADH Pool
Pyruvate
Lactate
ldhA
Formate Pathway
Pyruvate
pfl
Formate
Novel Pathway
Formate
?
Fe-Fe
H_2
CO_2
TR(M2) hyd
NADH Pool
Butyryl-CoA
Butanol
adhE, bdhA, bdhB
Butanol Pathway

Fig.S2

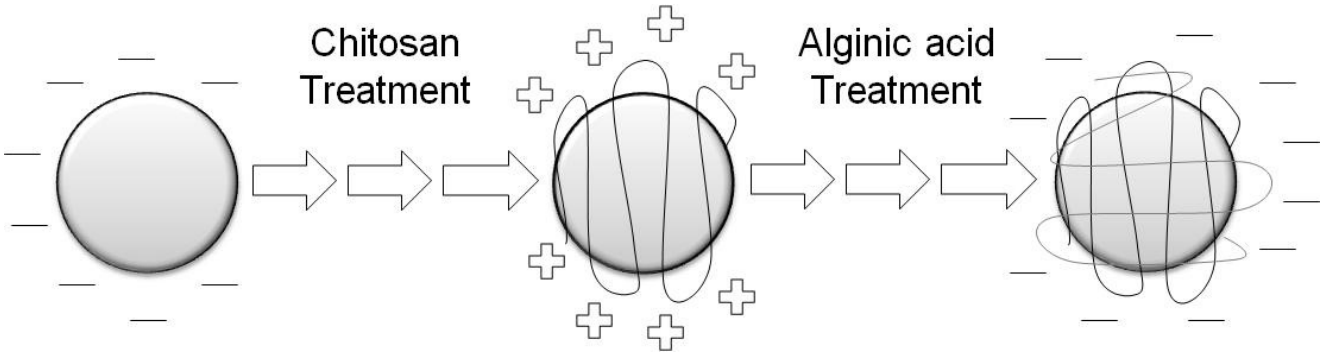

Fig.1

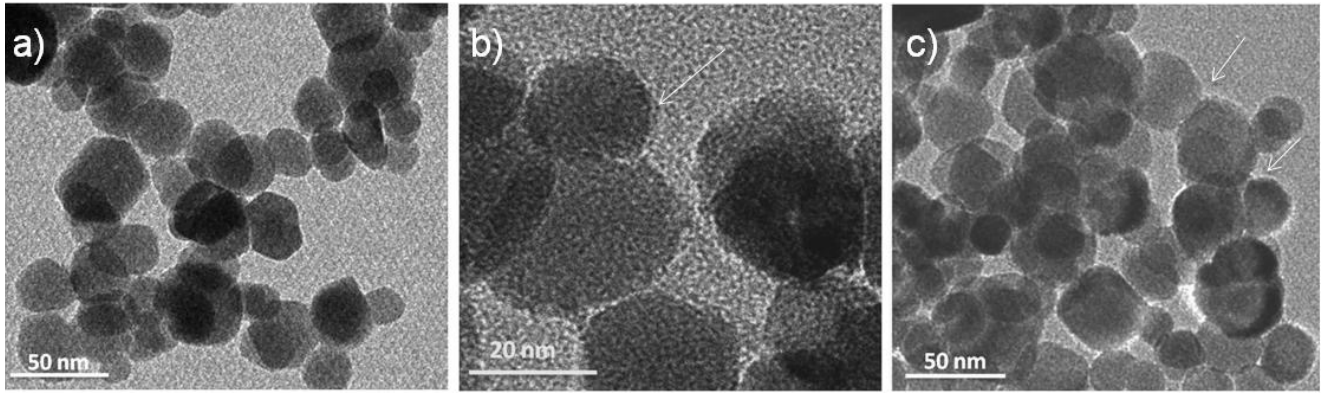

Fig.2a

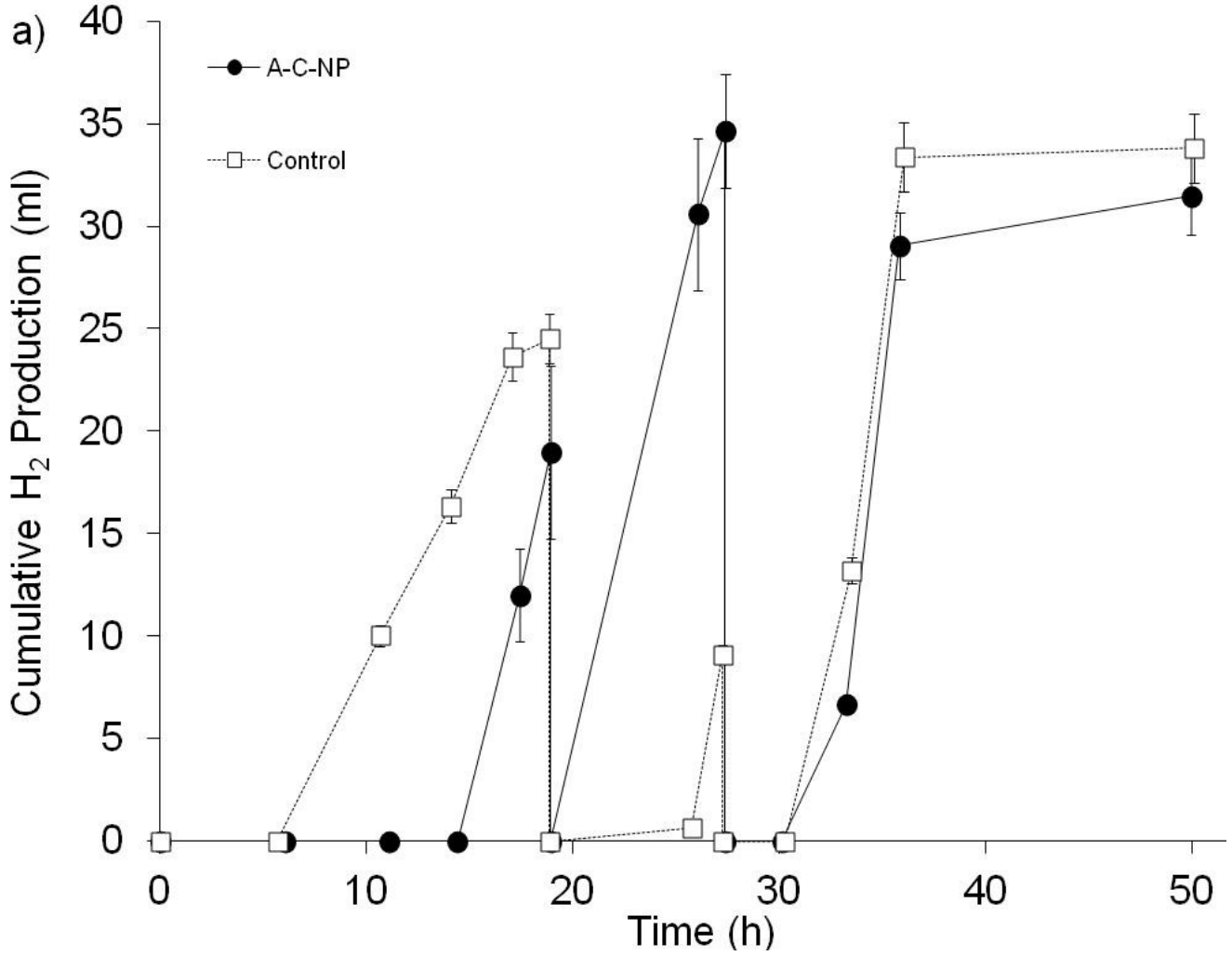
a)
A-C-NP
Control
Cumulative H_2 Production (ml)
0
5
10
15
20
25
30
35
40
0
10
20
30
40
50
Time (h)

Fig.2b

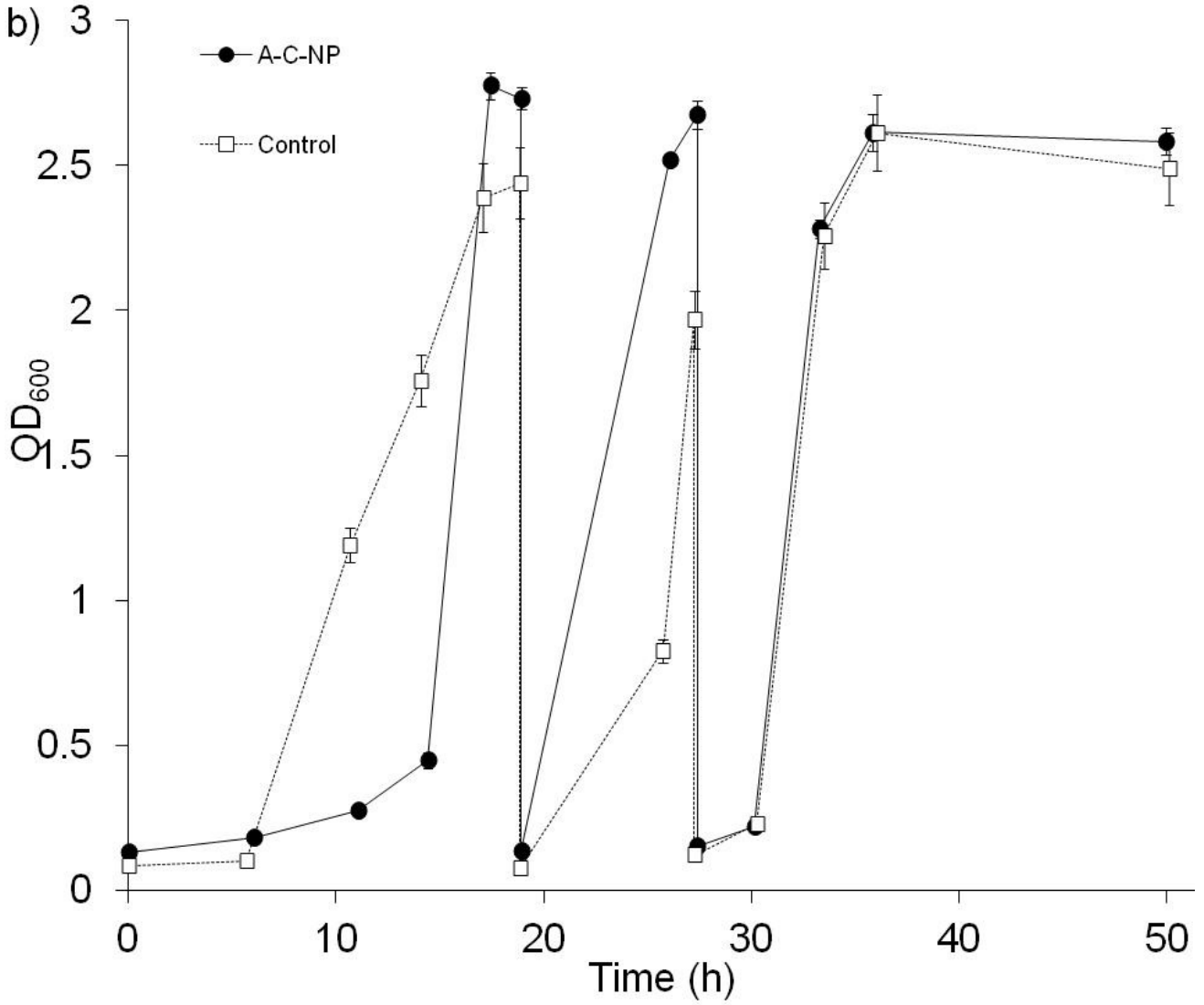

Fig.3

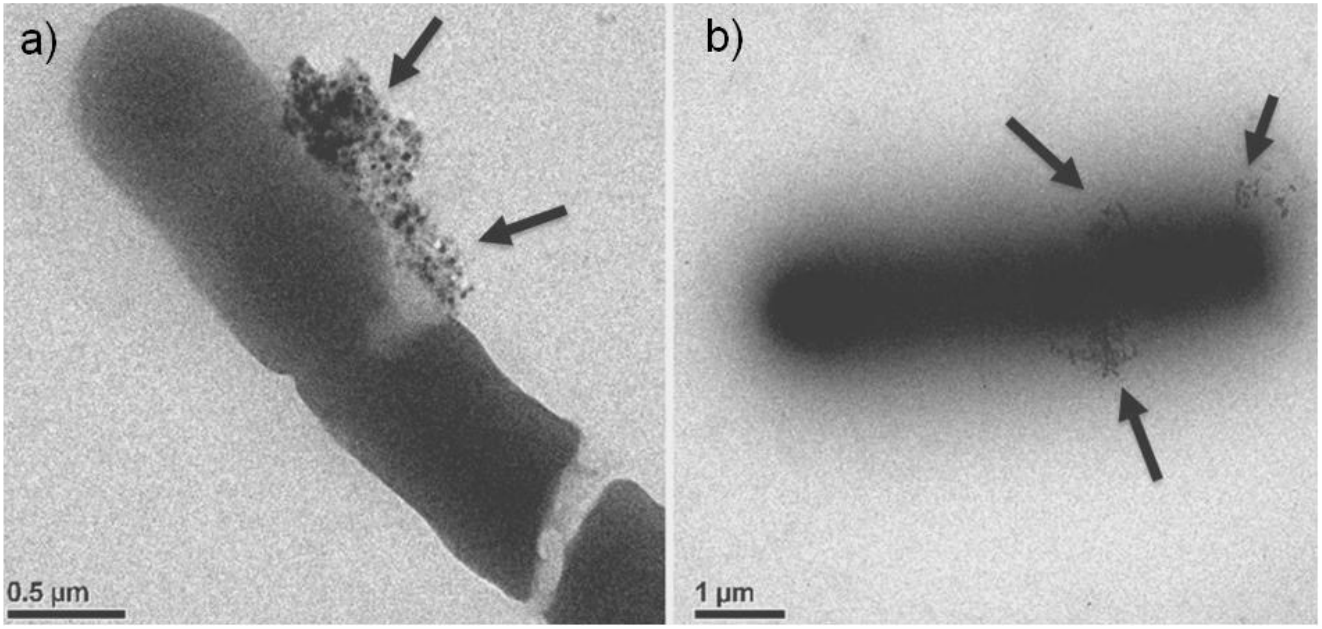

Fig.4

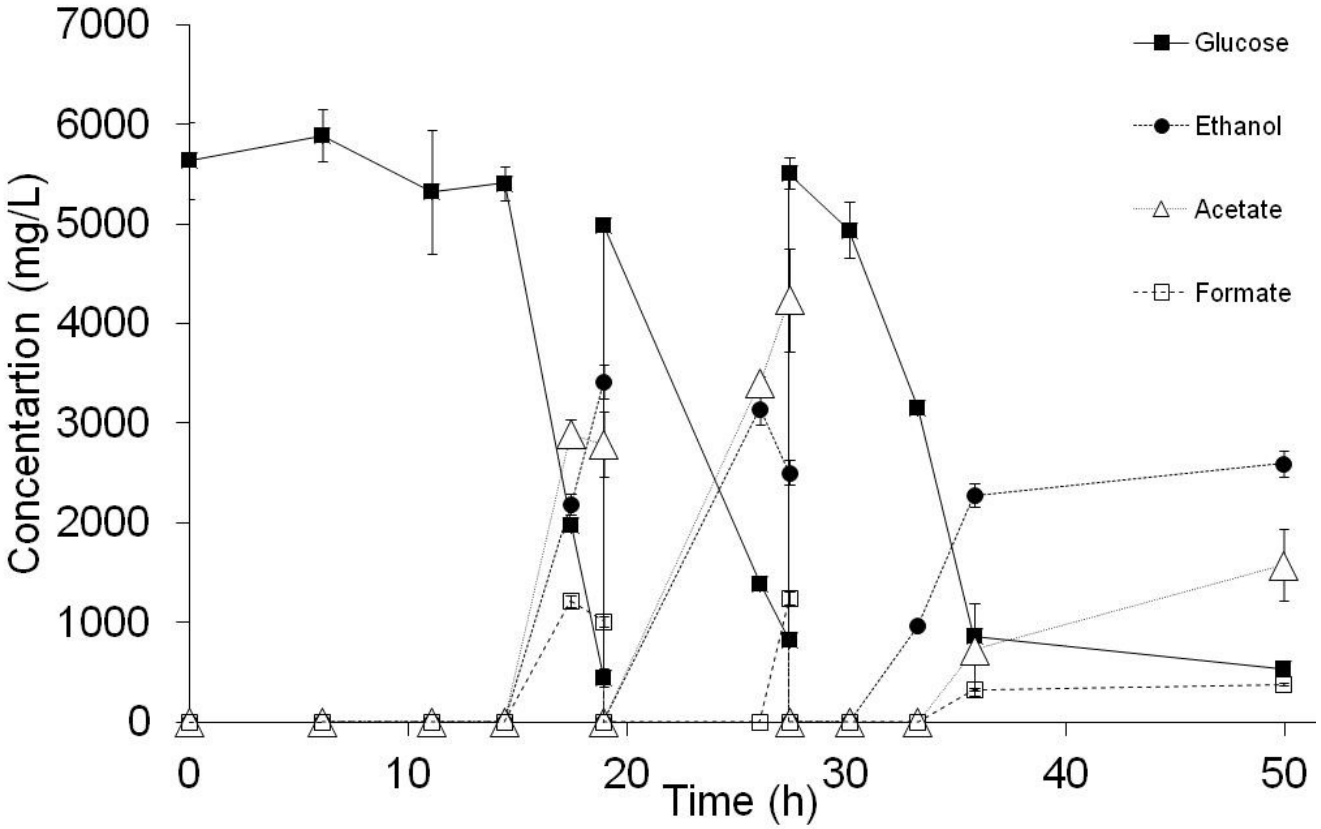
7000
6000
5000
4000
3000
2000
1000
0
Concentartion (mg/L)
0
10
20
30
40
50
Time (h)
Glucose
Ethanol
Acetate
Formate

Fig.5

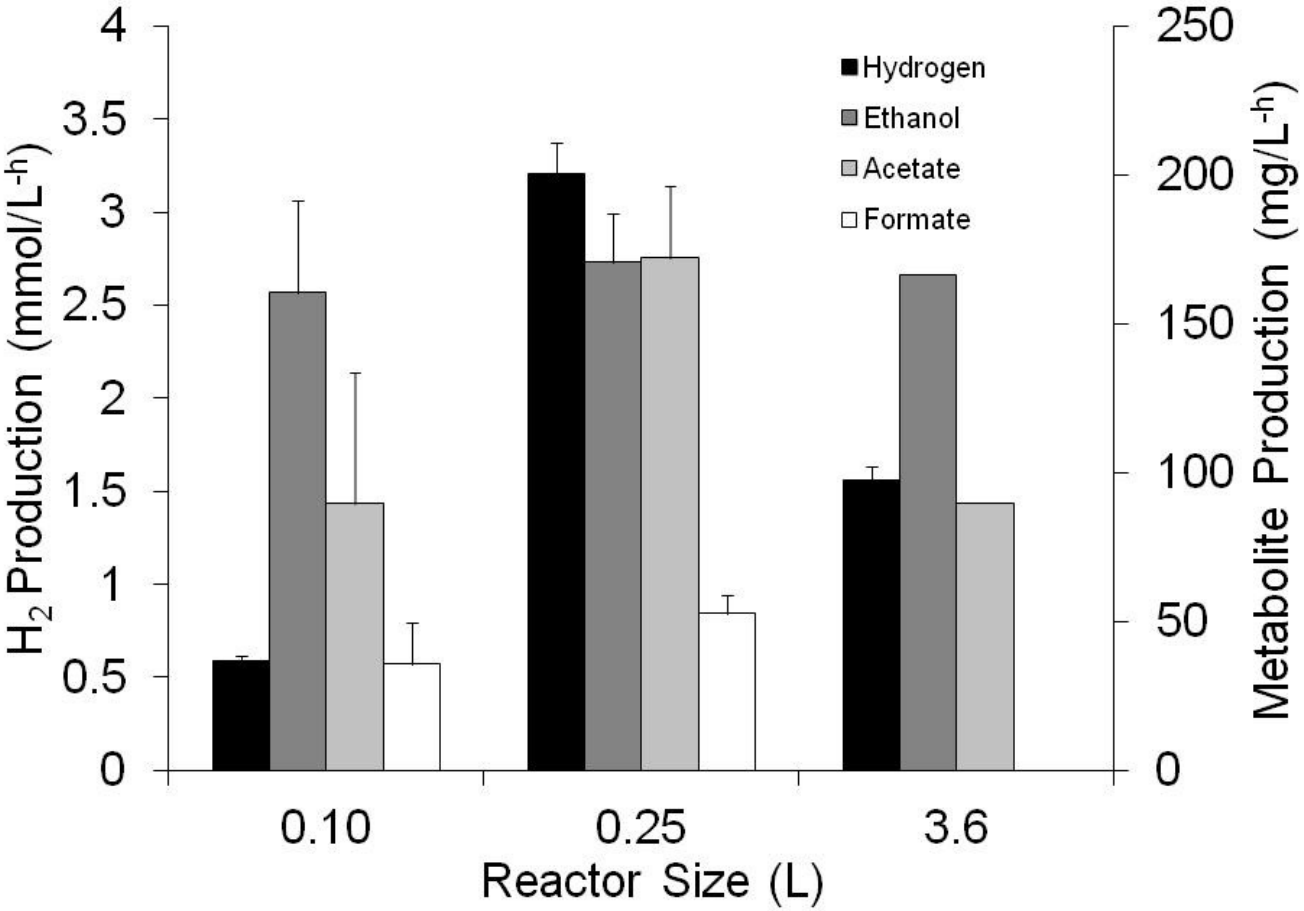
4
3.5
3
2.5
2
1.5
1
0.5
0
H_2 Production (mmol/L-h)
250
200
150
100
50
0
Metabolite Production (mg/L-h)
Hydrogen
Ethanol
Acetate
Formate
0.10
0.25
3.6
Reactor Size (L)

Fig.6

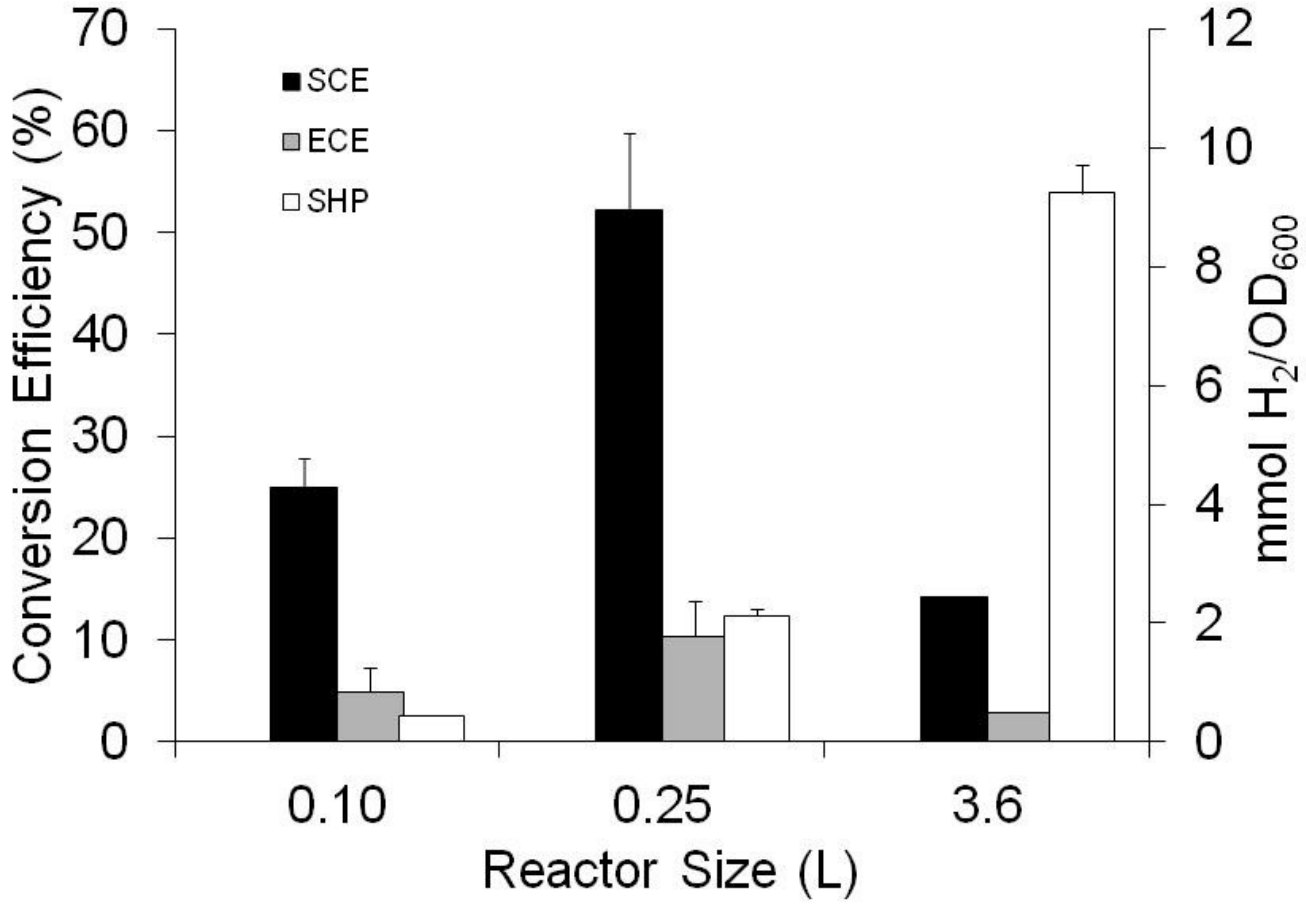
Conversion Efficiency (%)
70
60
50
40
30
20
10
0
SCE
ECE
SHP
12
10
8
6
4
2
0
mmol H_2/OD_{600}
0.10
0.25
3.6
Reactor Size (L)